Jpn. J. Appl. Phys. Vol. 41 (2002) pp. 3176–3180
Part 1, No. 5B, May 2002

Study on Ultrasonic Anomaly with Nonstoichiometry of Sintered Magnetite near Verwey Transition Temperature

Nobuo KASHIWAGURA, Shiun SAKAI and Hiroaki KAMIOKA
Faculty of Engineering, Gifu University, Yanagido, Gifu 501-1112, Japan

(Received November 19, 2001; accepted for publication January 4, 2002)

Compressional and shear wave velocities and attenuation in magnetite, which was sintered in N_2 gas atmosphere, were accurately measured to investigate the Verwey transition by the pulse transmission method using a dual acoustic path across the temperature range between 78 K and 300 K. The temperature dependence of the compressional and shear wave velocities of the sintered magnetite exhibited a depression at ~ 85 K. The low transition temperature corresponds to a large nonstoichiometry very close to the oxidation limit of magnetite. Using the measured ultrasonic data, the elastic properties of sintered magnetite are discussed. [DOI: 10.1143/JJAP.41.3176]

KEYWORDS: magnetite, Fe_3O_4, Verwey transition, nonstoichiometry, ultrasonic velocity, ultrasonic attenuation, elastic modulus, sintering

1. Introduction

At about 120 K, magnetite (Fe_3O_4) undergoes the well-known Verwey transition.[1)] For stoichiometric magnetite, the transition is of the first order and characterized by an abrupt change in electrical conductivity by a factor of $\sim 10^2$. To investigate the microscopic transition mechanism, research studies in comprehensive fields[2–6)] were carried out mainly on the magnetite single crystal. To date, it is believed that the transition is induced mainly by an ordering of the Fe ions on the octahedral sites in the low-temperature phase, but the detailed process is complicated.

Magnetite ($Fe_{3(1-\delta)}O_4$, $-0.0006 < \delta < 0.0125$) can take various states in the accessible stability range in "magnetite + hematite" phase depending on the oxygen amount during the heat processing condition. The nonstoichiometric deviation, i.e., the oxygen-to-iron ratio strongly affects not only the physical properties in the vicinity of the transition temperature but also the transition temperature itself.[7,8)] In the case of large nonstoichiometric deviation, $\delta > 0.004$, magnetite undergoes a second-order Verwey transition and does not exhibit any abrupt, discontinuous change in most physical properties including conductivity.[7,8)]

The main purpose of this study is to investigate the relationship between second-order Verwey transition and nonstoichiometry in magnetite ($Fe_{3(1-\delta)}O_4$). In the previous report, ultrasonic behavior with the second-order Verwey transition in the sintered magnetite, which lies near the oxidation limit, was reported.[9)] In this study, the acoustic property with the transition in the sintered magnetite, which lies very close to the oxidation limit, was measured and is compared with the previous one.

2. Experimental

Two samples with different degrees of nonstoichiometry were prepared. A schematic chart of sample preparation is shown in Fig. 1. Magnetite powder of 99.99% purity was formed into two cylindrical pellets. One of them (sample A) was sintered at the temperature of 1150°C in the atmosphere of slight vacuum of 6.7 Pa, and the other (sample B) was sintered in the atmosphere of N_2 gas flow. Characteristics of the two samples are listed in Table I.

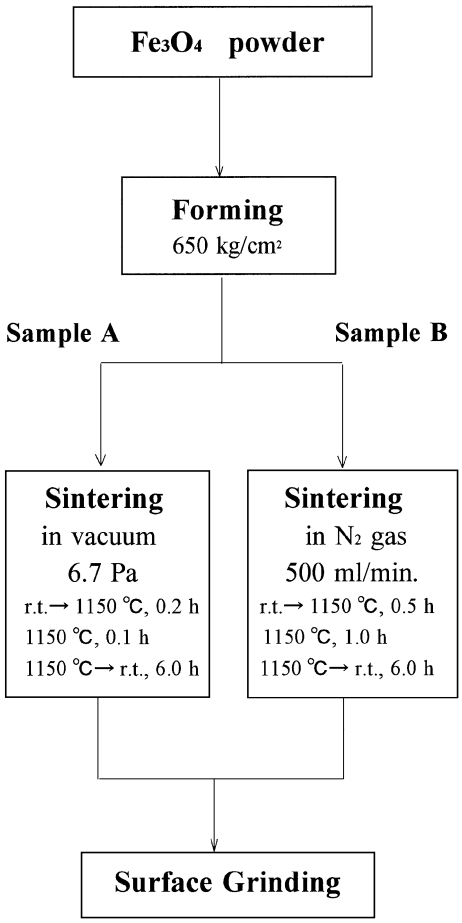

Fig. 1. Schema of sample preparation.

Temperature dependence of resistivity was measured using a four-probe method across the temperature range between 78 K and 300 K. The resistivity vs temperature curves for sample A and sample B are shown in Fig. 2. The resistivity curve for sample A, which was given in the previous report,[9)] is precisely measured again. As the temperature decreases, the resistivity curve for sample A does not exhibit any steep jump at around 120 K, but shows a slope change at around 138 K and small jumps at 116 K and at 94 K. The

Table I. Sample characteristics.

Name	Sample A	Sample B
Sintering atmosphere	in Vacuum of 6.7 Pa	in N_2 gas of 500 ml/min
Sintering temperature	1150°C	1150°C
Resistivity at 20°C	3.09×10^{-3} Ω·cm	3.24×10^{-2} Ω·cm
Density	4.36 g/cm^3	4.55 g/cm^3
Appearance	black	dark silver

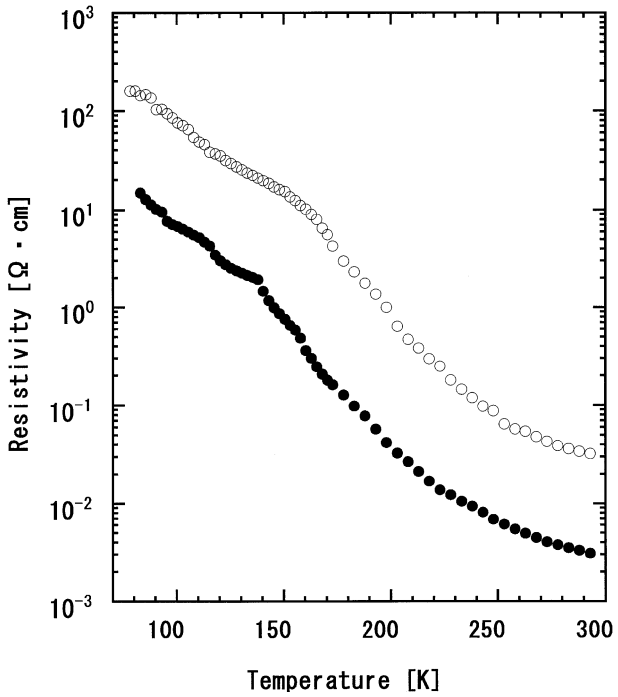

Fig. 2. Temperature dependence of resistivity. ●: sample A, ○: sample B.

small jump at ∼94 K corresponds to the second-order Verwey transition, and anomalies at ∼116 K and at ∼138 K are estimated to be a vestige and a foremonitored phenomena of the Verwey transition, respectively.[9] The resistivity at room temperature is higher by an order of 1.5 than that of a stoichiometric magnetite single crystal. The resistivity curve for sample B exhibits a similar temperature dependence, but the values are higher than that of sample A by an order of one at any temperature, and the curve shows small jumps at ∼88 K and ∼250 K. These characteristics of sample A and sample B are different from that of the stoichiometric magnetite single crystal, which exhibits an abrupt resistivity change at ∼120 K, but are probable for the large nonstoichiometric magnetite.[7]

For ultrasonic measurements, the pulse transmission method involving the use of a dual acoustic path was employed. The ultrasonic measurement was carried out in the same manner as that stated in the previous report.[9] The used measurement system is designed for precise ultrasonic measurement for small samples.[10,11] In this system, one path is the mercury delay line which is necessary for the precise measurement of ultrasonic velocity, and the other consists of the sample cell dipped in a liquid N_2 bath. The bath ensures a high heat capacity for the sample environment and the temperature of the sample cell is controlled by a microcomputer system. One MHz transducers were employed for both the compressional wave and shear wave measurements. Indium sheets, which are soft even at the liquid N_2 temperature, were used as acoustic binding materials.

3. Results and Discussion

Results of ultrasonic measurements and calculated elastic moduli for sample A have been reported in the previous paper.[9] In the following, results for sample B and comparison between sample A and sample B are shown.

3.1 Compressional wave

Ultrasonic measurements were carried out on the ceramic magnetite sample across the temperature range between 78 K and 300 K. The temperature dependence of compressional wave velocity V_c for sample B upon cooling and heating is shown in Fig. 3. There is slight hysteresis between the cooling and heating curves above 220 K. As the temperature decreases, V_c decreases gradually in the temperature range from 300 K to ∼100 K, it decreases abruptly in the range from ∼100 K to ∼85 K, and again increases steeply in the range from ∼85 K to 78 K. Consequently, the temperature dependence of V_c exhibits a sharp minimum at ∼85 K. The sharpness of the minimum is different between sample B and sample A.[9] Although the entire shape of the minimum is not obtained across the measured temperature range, the depth of depression and full-width at half minimum (FWHM) value can be roughly estimated by the "half" profile. The depth of the minimum is estimated to be ∼170 m/s and 250 m/s for sample B and sample A, respectively. The FWHM value is estimated to be 16°C and 11°C for sample B and sample A, respectively. The shape of the minimum of sample B is shallower and broader than that of sample A. In the measured temperature range, the absolute values of compressional wave velocity for sample B lie in the range from 5380 to 6010 m/s.

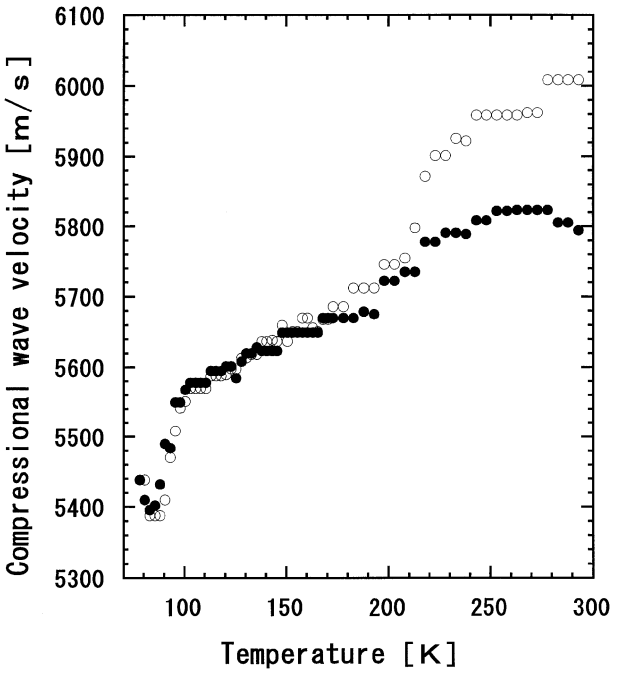

Fig. 3. Temperature dependence of 1 MHz compressional wave velocity for sample B. ●: upon cooling, ○: upon heating.

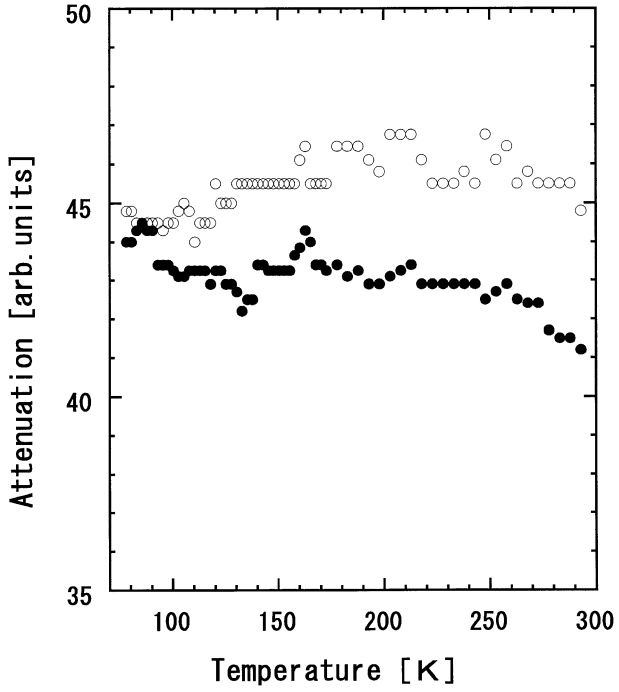

Fig. 4. Ultrasonic (1 MHz compressional wave) attenuation for sample B as a function of temperature. ●: upon cooling, ○: upon heating.

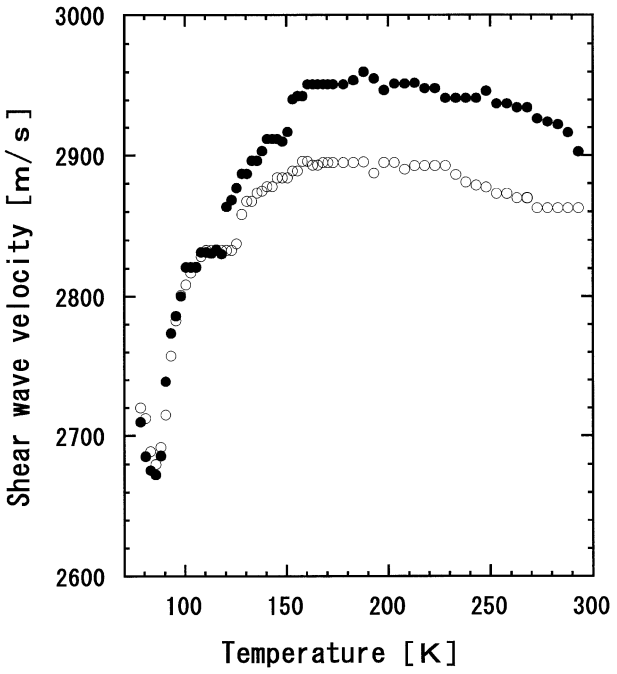

Fig. 5. Temperature dependence of 1 MHz shear wave velocity for sample B. ●: upon cooling, ○: upon heating.

These values are in almost the same range as that of sample A, and are significantly lower than that of $\sim 7.4 \times 10^3$ m/s for stoichiometric magnetite single crystals at room temperature. It appears that the low density, 4.55 g/cm^3, of the sample B affects the wave propagation: the density of stoichiometric magnetite single crystal is ~ 5.21 g/cm^3.

Figure 4 shows the temperature dependence of the compressional wave attenuation upon cooling and heating for sample B. There is a slight hysteresis between the cooling and heating curves. The attenuation upon heating has higher values than that upon cooling across the entire measured temperature range from 78 K to 300 K. Roughly speaking, the attenuation upon cooling has a slightly negative temperature coefficient, and the attenuation upon heating has a slightly positive temperature coefficient, across the measured temperature range. Furthermore, it is noted that small peaks at ~ 162 K and ~ 85 K and a small depression at ~ 132 K appear upon cooling, and that no significant peak, which consists of at least six dots per peak profile, but candidates for peaks at ~ 106 K, ~ 183 K, ~ 207 K and ~ 250 K appear upon heating.

3.2 Shear wave

The result of measurement of shear wave velocity, V_s, for sample B across the temperature range from 78 K to 300 K upon cooling and heating is shown in Fig. 5. As it is similar to the compressional wave velocity shown in Fig. 3, there is a slight hysteresis between the cooling and heating curves above ~ 120 K. As the temperature decreases, V_s increases in the temperature range from 300 K to ~ 190 K, decreases from ~ 190 K to ~ 120 K, stays constant from ~ 120 K to ~ 108 K, decreases rapidly from ~ 108 K to ~ 85 K, and again increases steeply in the range from ~ 85 K to 78 K. Consequently, the temperature dependence of V_s exhibits a sharp minimum at ~ 85 K. Similar to the case of a compressional wave, the sharpness of the minimum is different between sample B and sample A.[9] The depth of the minimum is estimated to be ~ 150 m/s and ~ 90 m/s for sample B and sample A, respectively. The FWHM value is estimated to be 16°C and 11°C for sample B and sample A, respectively. The shape of the minimum of sample B is deeper and broader than that of sample A. In the measured temperature range, the absolute values of compressional wave velocity for sample B lie in the range from 2670 to 2960 m/s. These values are significantly lower than that of sample A.

Comparing Figs. 3 and 5, it is noted that the shapes of the minimums of V_c and V_s at ~ 85 K are very similar. Because of the sample preparation, the nonstoichiometry of the sample B is larger than that of sample A, the transition temperature of which was estimated to be ~ 90 K.[9] It was demonstrated by heat capacity investigation that the larger stoichiometric deviation results in a lower transition temperature for the Verwey transition.[8] The temperature of the Verwey transition for sample B is expected to be less than ~ 90 K. Thus, the Verwey transition temperature of sample B is estimated to be ~ 85 K. The transition temperature, ~ 85 K, is considerably low in comparison to ~ 120 K for a stoichiometric magnetite, Fe_3O_4, single crystal. It has previously been demonstrated by heat capacity[8] and thermoelectric power[7] measurements that the Verwey transition temperature of a nonstoichiometric magnetite, $Fe_{3(1-\delta)}O_4$, decreases considerably with respect to the stoichiometric deviation, δ. According to the heat capacity investigation,[8] sample B is presumed to be nonstoichiometric by an amount of ~ 0.011 in δ. The stoichiometric deviation, $\delta \sim 0.011$, corresponds to the magnetite which lies very close to the oxidation limit, $\delta = 0.0125$. Whereas sample A, which was subjected to heat treatment in a slight vacuum atmosphere of 6.7 Pa, is presumed to be nonstoichiometric with δ of ~ 0.009 (given as ~ 0.01 in ref. 9, but re-estimated precisely). The δ value corresponds to the magnetite near the oxidation limit. For such large deviations near the oxidation limit, the Verwey transition can no longer be of the first order,

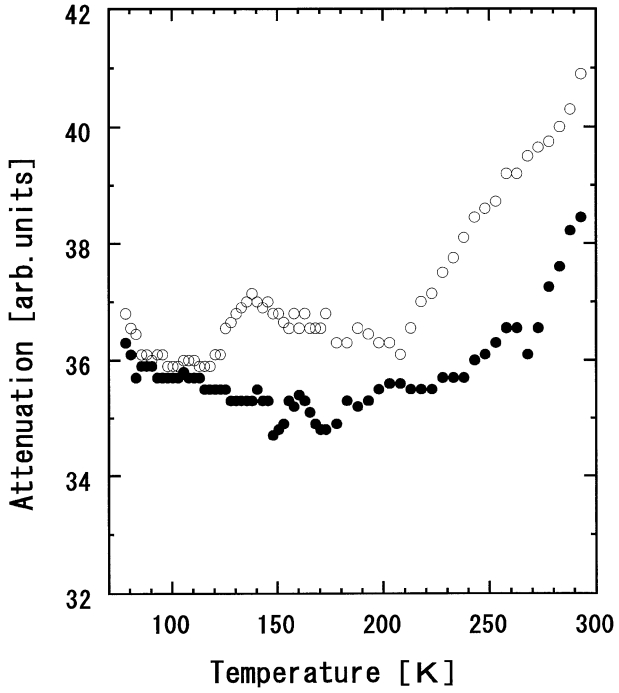

Fig. 6. Ultrasonic (1 MHz shear wave) attenuation for sample B as a function of temperature. ●: upon cooling, ◯: upon heating.

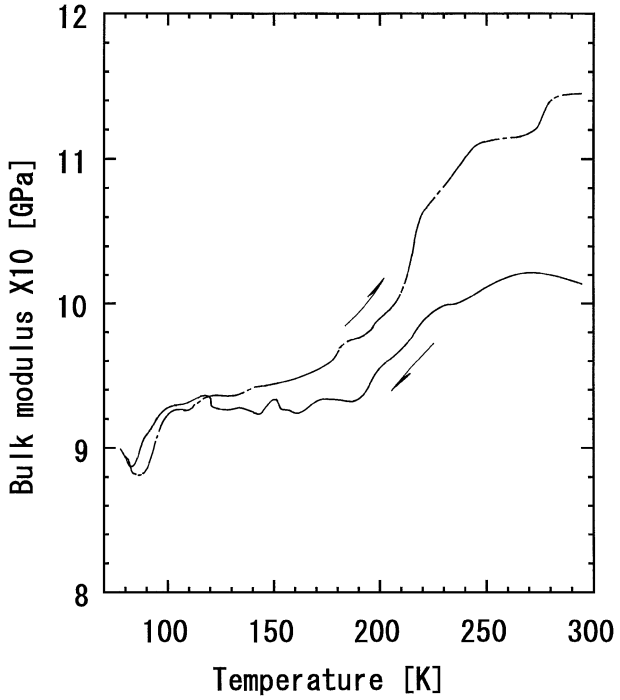

Fig. 7. Temperature dependence of bulk modulus for sample B. Curve marked with "←": upon cooling, curve marked with "→": upon heating.

but is that of the second order.[8)]

The temperature dependence of electrical resistivity for sample B exhibits small jumps at ∼88 K and ∼250 K as shown in Fig. 2. As for the small jump at ∼250 K, there is no corresponding anomaly in ultrasonic data, and the temperature, ∼250 K, is highly deviated from the expected region, ∼120 K or less, for Verwey transition.[8)] Thus, the small jump at ∼250 K may correspond to a change of state other than Verwey transition. The small change in resistivity at ∼88 K is not contradictory to the Verwey transition of second order. Although the resistivity anomaly for the second-order Verwey transition is small, the ultrasonic anomaly is highly apparent. It is presumed that the second-order Verwey transition as a structural phase transition affects more the phonon state than the electronic state. The transition temperature in resistivity, ∼88 K, is slightly different from that in ultrasonic measurement, ∼85 K. To interpret the discrepancy, detailed investigation is necessary.

Figure 6 shows the temperature dependence of shear wave attenuation upon cooling and heating. Similar to the compressional wave attenuation, a slight hysteresis exists between the cooling and heating curves, and the attenuation upon heating has higher values than that upon cooling over the entire measured temperature range from 78 K to 300 K. In contrast to the compressional wave attenuation, the shear wave attenuation upon both heating and cooling roughly shows a concave shape across the measured temperature range.

3.3 Elastic moduli

In order to investigate the elastic property, it is necessary to calculate the elastic moduli. Using the values of the compressional wave velocity, V_c, and the shear wave velocity, V_s, given in Figs. 3 and 5, respectively, the elastic moduli for sample B are computed using equations[9)] and their temperature dependence is illustrated in Fig. 7 (bulk modulus), Fig. 8

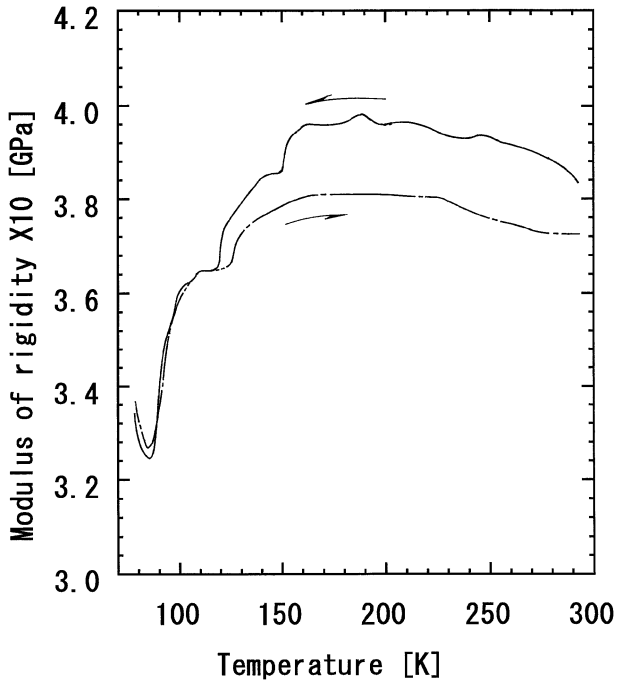

Fig. 8. Modulus of rigidity for sample B as a function of temperature.

(modulus of rigidity), Fig. 9 (Young's modulus) and Fig. 10 (Poisson's ratio). The cooling and the heating curves are distinguished by the lines and arrows which indicate the directions of temperature change.

From Figs. 7–10, it is noted that: 1) bulk modulus, modulus of rigidity and Young's modulus exhibit a distinct depression at ∼85 K; 2) Poisson's ratio exhibits a peak at ∼85 K; 3) modulus of rigidity and Young's modulus exhibit a similar temperature dependence across the measured temperature region from 300 K to 78 K; and 4) only Poisson's ratio has

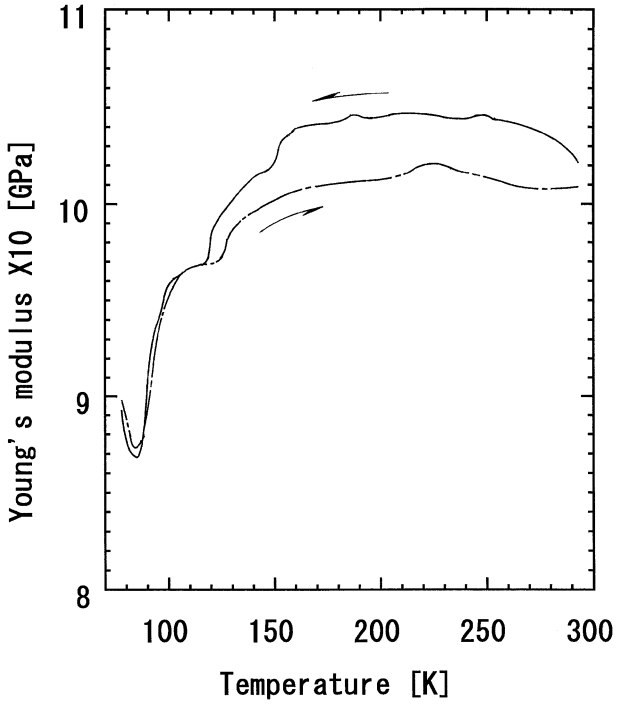

Fig. 9. Temperature dependence of Young's modulus for sample B.

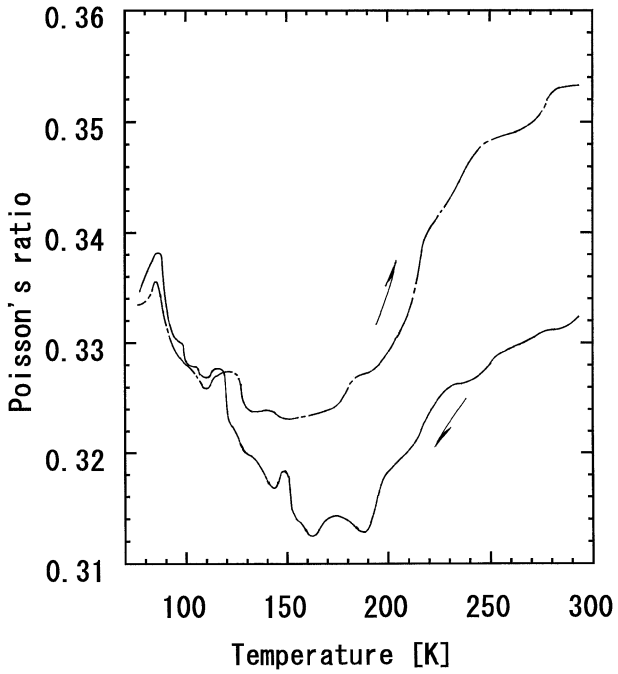

Fig. 10. Poisson's ratio for sample B as a function of temperature.

a concave shape over the entire temperature range. The features, 1) and 2), suggest that sample B undergoes the second-order Verwey transition at $\sim$ 85 K, and accordingly the elastic property changes markedly.

In comparison between elastic moduli for sample B and that for sample A, it is also noted that: 5) the bulk modulus for sample B is significantly higher than that for sample A; 6) the modulus of rigidity for sample B is considerably lower than that for sample A; 7) the Young's modulus for sample B is considerably lower than that for sample A; 8) The temperature dependence of Poisson's ratio for sample B is quite different from that for sample A. As a whole, the changes in elastic moduli with second-order Verwey transition for sample B are more moderate than those of sample A.

4. Conclusions

The ultrasonic wave method was applied to investigate the Verwey transition in sintered magnetite across the temperature range from 78 K to 300 K, and the following information was obtained.

1) The magnetite, which was treated in N_2 gas, undergoes the second-order Verwey transition at $\sim$ 85 K, and the nonstoichiometry parameter, δ, is estimated to be $\sim$ 0.011.

2) The magnetite, which was treated in a slight vacuum of 6.7 Pa, undergoes the second-order Verwey transition at $\sim$ 90 K, and the nonstoichiometry parameter, δ, is estimated to be $\sim$ 0.009.

3) The larger the nonstoichiometry deviation becomes, the more moderate is the change in the acoustic property, with the second-order Verwey transition.

1) E. J. W. Verwey and P. W. Haayman: Physica (Utrecht) **8** (1941) 979.
2) J. P. Shepherd, J. W. Koenitzer, R. Aragon, C. J. Sandberg and J. M. Honig: Phys. Rev. B **31** (1985) 1107.
3) C. Constantin and M. Rosenberg: Solid State Commun. **9** (1971) 675.
4) M. Rubinstein and D. W. Forester: Solid State Commun. **9** (1971) 1675.
5) R. S. Hargrove and W. Kundig: Solid State Commun. **8** (1970) 303.
6) E. J. Samuelsen, E. J. Bleeker, L. Dobrzynski and T. Riste: J. Appl. Phys. **39** (1968) 1114.
7) A. J. M. Kuipers and V. A. M. Brabers: Phys. Rev. B **14** (1976) 1401.
8) J. P. Shepherd, J. W. Koenitzer, R. Aragon, J. Spalek and J. M. Honig: Phys. Rev. B **43** (1991) 8461.
9) N. Kashiwagura, S. Sakai and H. Kamioka: Jpn. J. Appl. Phys. **40** (2001) 3516.
10) H. Kamioka: Jpn. J. Appl. Phys. **36** (1997) 2896.
11) N. Kashiwagura, Y. Ohsawa, S. Iwata, J. Jin and H. Kamioka: Jpn. J. Appl. Phys. **39** (2000) 2928.